The Astrophysical Journal, 712:429–434, 2010 March 20 doi:10.1088/0004-637X/712/1/429

RELATING CORONAL MASS EJECTION KINEMATICS AND THERMAL ENERGY RELEASE TO FLARE EMISSIONS USING A MODEL OF SOLAR ERUPTIONS

Katharine K. Reeves[1] and Stephanie J. Moats[1,2]
[1] Harvard-Smithsonian Center for Astrophysics, 60 Garden St., MS 58, Cambridge, MA 02138, USA; kreeves@cfa.harvard.edu
[2] New Mexico Institute of Mining and Technology, 801 Leroy Pl, Socorro, NM 87801, USA
Received 2009 December 15; accepted 2010 February 4; published 2010 March 2

ABSTRACT

We use a model of solar eruptions that combines a loss-of-equilibrium coronal mass ejection (CME) model with a multi-threaded flare loop model in order to understand the relationship between the CME kinematics, thermal energy release, and soft X-ray emissions in solar eruptions. We examine the correlation between CME acceleration and the peak soft X-ray flux in many modeled cases with different parameters, and find that the two quantities are well correlated. We also examine the timing of the peak acceleration and the light curve derivative, and find that these quantities tend to peak at similar times for cases where the magnetic field is high and the inflow Alfvén Mach number is fast. Finally, we study the relationship between the total thermal energy released in the model and the calculated peak soft X-ray flux of the resulting flare. We find that there is a power-law relationship between these two quantities, with $F_{\rm peak} \sim E^{\alpha}$, where α is between 2.54 and 1.54, depending on the reconnection rate. This finding has repercussions for the assumptions underlying the Neupert effect, in which the peak soft X-ray flux is assumed to be proportional to the thermal energy release.

Key words: Sun: coronal mass ejections (CMEs) – Sun: flares

1. INTRODUCTION

Reconnection has long been assumed to be the driver behind both flares and coronal mass ejections (CMEs; e.g., Harrison 2003). As a consequence, there should be a connection between the kinematics of CMEs and the light curve of the associated flare. Several studies have found correlations between CME speeds and the peak flare emissions (Moon et al. 2002; Burkepile et al. 2004; Vršnak et al. 2005). Correlations have also been found between the peak acceleration of the CME and the peak soft X-ray flux of the resulting flare (Maričić et al. 2007). Many studies have looked at the timing of these quantities to discover the nature of the connection, and have found that there is often a correlation between the CME (or filament) acceleration and the derivative of the light curve of the associated flare (e.g., Gallagher et al. 2003; Vršnak et al. 2004; Qiu et al. 2004; Zhang et al. 2004; Jing et al. 2005; Sterling & Moore 2005; Maričić et al. 2007).

The assumption made in the conclusions of the above observational studies is that the energy released during the eruption should be correlated with the CME acceleration as well as the derivative of the flare light curve. We investigated the first part of this assumption previously (Reeves 2006) by examining the relationship between the CME acceleration and the energy release in a loss-of-equilibrium CME model. We found that the peaks of the CME acceleration and energy release were nearly co-temporal only if the background magnetic field is high and the reconnection rate is fast.

The relationship between the energy release in the flare and the resulting X-ray light curve is not necessarily straightforward, however. There is growing consensus in the solar community that solar flares consist of multi-threaded arcades, with loops energized at different times (e.g., Hori et al. 1997, 1998; Aschwanden & Alexander 2001; Reeves & Warren 2002; Warren & Doschek 2005; Warren 2006; Reeves et al. 2007). In our previous work (Reeves 2006), we surmised that this multi-threaded nature of flares would complicate the relationship between the energy release and the flare light curve.

An observational manifestation of the relationship between the energy release in flares and the resulting light curves known as the Neupert effect relates the time-integrated microwave intensity and the peak soft X-ray flux (Neupert 1968). Hard X-rays often show the same relationship with soft X-rays, since they are produced by the same population of non-thermal particles as microwaves. This relationship implies that the peak soft X-ray flux is proportional to the total thermal energy input into the flare, and that the hard X-rays are proportional to the energy deposition rate (Lee et al. 1995). However, modeling done by Warren & Antiochos (2004) indicates that the hydrodynamic response of a single loop is not consistent with proportionality between peak soft X-ray flux and thermal energy. They speculate that combining many hydrodynamic loops into one flare arcade may resolve this discrepancy.

In this paper, we examine the relationship between the CME kinematics and the soft X-ray flare emissions using a model of solar eruptions that combines a loss-of-equilibrium CME model with multi-threaded flare loop modeling. We also study the relationship between the thermal energy release in this model and the peak soft X-ray flux, and detail the implications for observations that exhibit the Neupert effect. The model we use is described in Section 2. We present our results in Section 3, and the discussion and conclusions are presented in Section 4.

2. DESCRIPTION OF THE MODEL

We use a loss-of-equilibrium model based on that of Lin & Forbes (2000) that has been used previously to determine the thermal energy input into multi-threaded flare models (Reeves & Forbes 2005; Reeves et al. 2007). In this model, a flux rope begins in equilibrium with the forces due to magnetic tension, magnetic compression, and gravity balancing each other. The flare footpoints are moved together quasi-statically until there is no longer a possible equilibrium state for the flux rope, and an eruption occurs. After the loss of equilibrium, a current sheet forms underneath the flux rope, and flare loops are formed by the reconnecting magnetic fields. The magnetic field configurations before and after the eruption are shown in Figure 1.

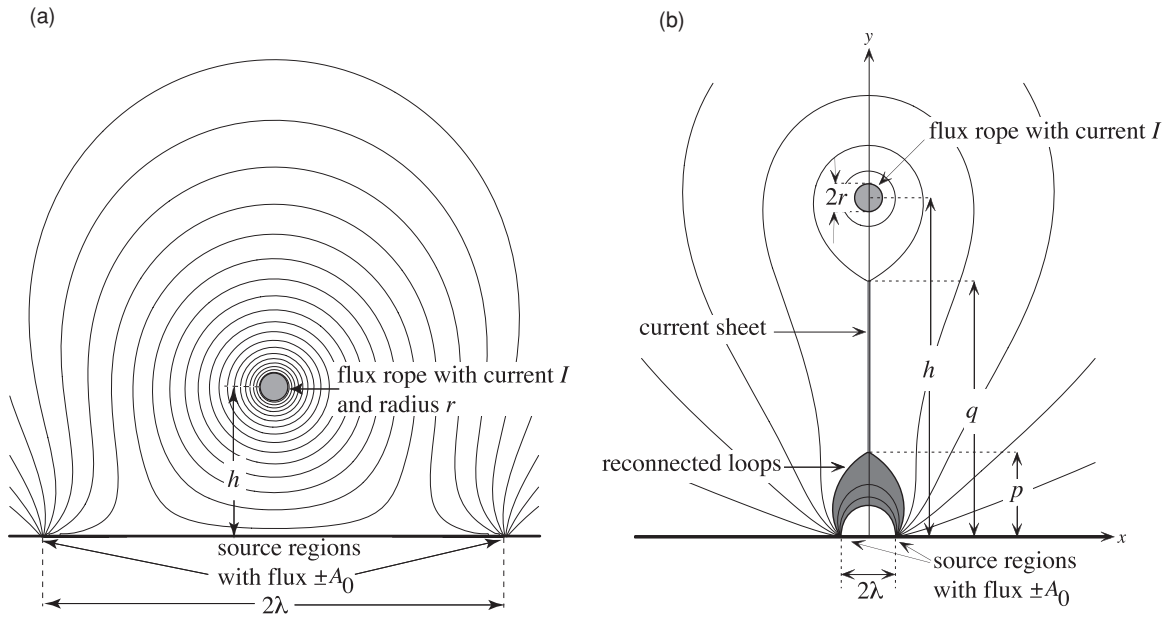

Figure 1. (a) Magnetic configuration for the model prior to the loss of equilibrium. The current, I, is in the z-direction, out of the plane of the figure. (b) Magnetic configuration for the model after the eruption and formation of the current sheet. From Reeves (2006).

In this model, we assume that all of the energy swept into the current sheet via the Poynting flux is converted into thermal energy. Thus, the thermal energy release rate in this model is found by integrating the Poynting flux over the length of the current sheet:

$$\frac{dW_{\rm th}}{dt} = \frac{c}{2\pi} E_z(t) \int_{p(t)}^{q(t)} B_y(0, y, t) dy. \quad (1)$$

In the equation above, q and p represent the top and bottom tips of the current sheet, respectively, as shown in Figure 1(b). We assume that half of this energy is directed upward toward the escaping CME and half is directed downward toward the flare loops. The electric field, E_z, is given by

$$E_z = -\frac{1}{c}\frac{\partial A_{cs}}{\partial t} = M_A V_A(0, y_0) B_y(0, y_0)/c, \quad (2)$$

where $A_{\rm cs} = A(0, p \leqslant y \leqslant q)$ is the magnitude of the vector potential along the current sheet. We set the inflow Alfvén Mach number, M_A, to a constant at the midpoint of the current sheet (y_0). The Alfvén speed, V_A, and the magnetic field, B_y, are evaluated at y_0. M_A provides a measure of the reconnection rate in the current sheet, since it is directly proportional to E_z.

Previous work has used the thermal energy release from this model to determine the energy input into an arcade of multi-stranded flare loops (Reeves & Forbes 2005; Reeves et al. 2007). Reeves & Forbes (2005) used a 0D model to calculate temperatures and densities in the loops based on the calculations of Cargill et al. (1995), and found that the model produced soft X-ray light curves commensurate with observations. In this work, we use the Enthalpy-Based Thermal Evolution of Loops (EBTEL) model developed by Klimchuk et al. (2008), who found that this model calculates the evolution of the average temperature, pressure, and density in a coronal loop in agreement with more sophisticated (and computationally intensive) one-dimensional (1D) hydrodynamic calculations. The EBTEL model solves the following equations for the average pressure ($\bar{P}$), density ($\bar{n}$), and temperature ($\bar{T}$) along the loop:

$$\frac{d\bar{P}}{dt} \approx \frac{2}{3}\left(\bar{Q} - \frac{1}{L}(R_c + R_{tr})\right) \quad (3)$$

$$\frac{d\bar{n}}{dt} = -\frac{c_2}{5c_3 k L \bar{T}}(F_0 + R_{tr}) \quad (4)$$

$$\frac{d\bar{T}}{dt} \approx \bar{T}\left(\frac{1}{\bar{P}}\frac{d\bar{P}}{dt} - \frac{1}{\bar{n}}\frac{d\bar{n}}{dt}\right). \quad (5)$$

In the equations above, $\bar{Q}$ is the spatial average of the volumetric heating rate, L is the total length of the loop, R_c and R_{tr} are the radiative cooling rates per unit cross-sectional area in the corona and the transition region, respectively, c_2 is the ratio of the average temperature to the apex temperature ($\bar{T}/T_a$), c_3 is the ratio between the coronal base temperature and apex temperature (T_0/T_a), k is Boltzmann's constant, and F_0 is heat flux at the base of the corona. We take c_2 to be 0.87, c_3 to be 0.7, and R_{tr}/R_c to be 4.0, as in Klimchuk et al. (2008).

We determine the volumetric heating rate, $\bar{Q}$, by partitioning the thermal energy output by the loss-of-equilibrium model into an arcade of several hundred loops. This energy partitioning is done in the same manner as in Reeves et al. (2007), where the energy pulses are assumed to be triangular in time, and their peak energy is determined by the thermal energy output of the loss-of-equilibrium model. The heat input is assumed to be a Gaussian function of space, centered on the apex of the loop with a width of 10^8 cm. More details on this energy partitioning can be found in Reeves et al. (2007). We also assume a background heating in each loop such that the loop is initially in thermal equilibrium at 1 MK. The value of this background heating is calculated in accordance with the scaling laws of Serio et al. (1991).

We assume that the loops are formed every 20 s, and there are approximately 500 loops for each simulated flare. From the temperatures and densities in these loops, we calculate the intensity that would be observed in the *Geostationary Operational Environmental Satellite* (*GOES*) 1–8 Å channel,

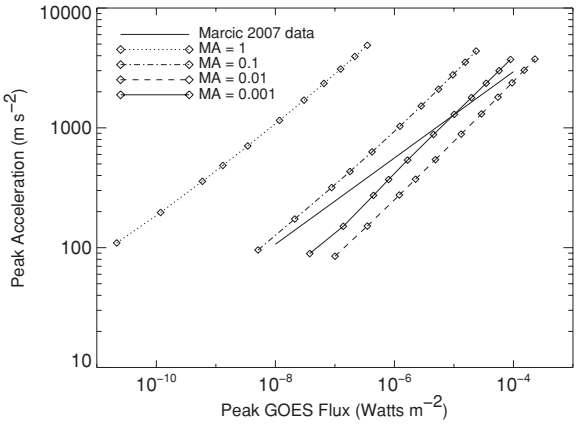

Figure 2. Peak acceleration of the flux rope vs. the peak *GOES* flux for all the cases studied. Diamonds indicate the value of the background magnetic field for each case. The Mach numbers for the curves are 1 (dotted line), 0.1 (dash-dotted line), 0.01 (dashed line), and 0.001 (solid line). Also included is a fit to data found by Maričić et al. (2007; solid line with no symbols).

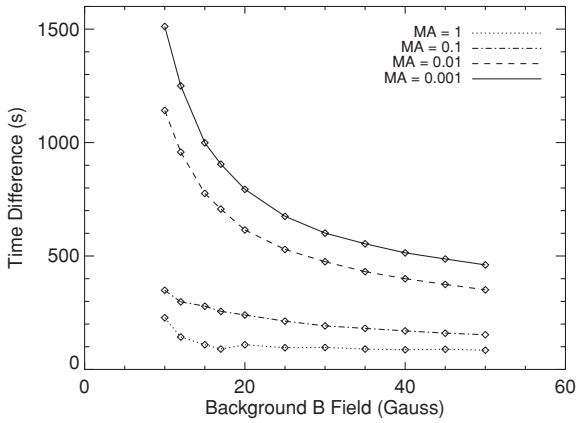

Figure 3. Time difference between the peaks of the acceleration of the flux rope and the light curve derivative for all the cases studied. Positive numbers indicate that the peak in the acceleration leads the peak in the light curve derivative. Diamonds indicate the value of the background magnetic field for each case. Line styles are the same as in Figure 2.

using the SolarSoft routine `goes_fluxes`. The geometry of the loops, i.e., the length and thickness of the loops, is determined by the magnetic field model, and the arcade length (i.e., the length out of the page in Figure 1) is 10^{10} cm.

The width of the triangular heating pulse in each loop is assumed to be 40 s. We also calculated cases where this heating window is 20, 80, and 200 s, and found that the width of the heating window does not significantly affect the *GOES* light curve. This result is consistent with the results of Warren (2006) who found that for a multi-stranded flare made up of 1D hydrodynamically modeled loops, the width of the heating window affects channels that detect the highest temperature emission, such as the M1 channel on Yohkoh's Hard X-Ray Telescope, but the *GOES* emission is not significantly changed by varying the width of the heating function.

3. RESULTS

3.1. Relationship Between CME Kinematics and Soft X-ray Emissions

For this study, we use the same parameters as in Reeves (2006): the length scale h_0 (given by the height of the flux rope in equilibrium when its current is maximized) is 5×10^9 cm, the mass per unit length of the flux rope is 2.1×10^6 g cm^{-1}, and the density at the base of the corona is 1.67×10^{-16} g cm^{-3}. We vary the background magnetic field between 10 G and 50 G, and we vary M_A between 0.001 and 1. Observations typically place the reconnection rate in the range of 0.001–0.1 (e.g., Dere 1996; Isobe et al. 2005; Lin et al. 2005), but we include $M_A = 1$ in order to investigate the limits of the calculation over a wide range of reconnection rates.

Figure 2 shows the relationship between the peak acceleration and the peak *GOES* 1–8 Å flux for all of the cases studied. We find that for each value of M_A, there is a power-law relationship between the acceleration and the peak *GOES* flux, with an index varying between 0.39 for the $M_A = 1$ cases and 0.49 for the $M_A = 0.001$ cases. In this model, increasing the reconnection rate increases the fraction of the total energy that goes into thermal heating (Reeves & Forbes 2005), thus increasing the peak *GOES* flux and accounting for the shift of the lines to the right as M_A decreases in Figure 2. The obvious exception to this trend is the case with the slowest reconnection rate, $M_A = 0.001$. In the model, the thermal energy must go to zero as $M_A \rightarrow 0$, since the Poynting flux into the current sheet is zero in that case. For the parameters used in this model, $M_A = 0.001$ is beyond the threshold where the fractional thermal energy is maximized. A further discussion of the effect of the reconnection rate on the energy release in this model can be found in Reeves & Forbes (2005).

In Figure 2, we also plot the relationship between the peak acceleration and the peak *GOES* flux found by Maričić et al. (2007) from observations of CMEs and their associated flares. They find that there is a power-law relationship between the peak CME acceleration and the peak *GOES* flux, though their index of 0.36 is slightly lower than the modeled cases due to the scatter in the data. From this plot, it is easy to see that the reconnection rate is likely to contribute to the scatter in the observations.

The timing between the acceleration of the flux rope and the rise in the soft X-ray light curve is also an important metric that has been investigated observationally. Many studies find good correlations between the evolution of the acceleration curve and the derivative of the soft X-ray light curve (Vršnak et al. 2004; Qiu et al. 2004; Zhang et al. 2004; Maričić et al. 2007), though there are certainly cases where good agreement is not found (e.g., the weak field case in Zhang et al. 2001 or the B7.2 flare in Maričić et al. 2007). Figure 3 shows the difference in time between the peak of the flux rope acceleration and the peak in the derivative of the soft X-ray light curve for each of the simulated cases studied. This plot shows that a decrease in the reconnection rate of the eruption tends to increase the time between the peak CME acceleration and the peak in the derivative of the soft X-ray flux. This effect is much more pronounced for the cases with weaker magnetic fields.

Figure 4 shows the acceleration and the derivative of the light curve for two cases, one where the peaks of these two curves are the closest in time ($M_A = 1$, $B = 50$ G, Figure 4(a)) and the other where the peaks of the two curves are the farthest in time ($M_A = 0.001$, $B = 10$ G, Figure 4(b)). In the case where the peaks are closest together, they are separated by about 100 s. For the case where the peaks are the farthest apart, they are almost 1500 s apart. The weakest flare studied by Maričić et al. (2007), a B7.2 flare that occurred on 2003 February 18, has a peak in the derivative of the soft X-ray light curve several tens of minutes after the peak in the acceleration of the CME, indicating that such a temporal gap between the peak acceleration and the peak

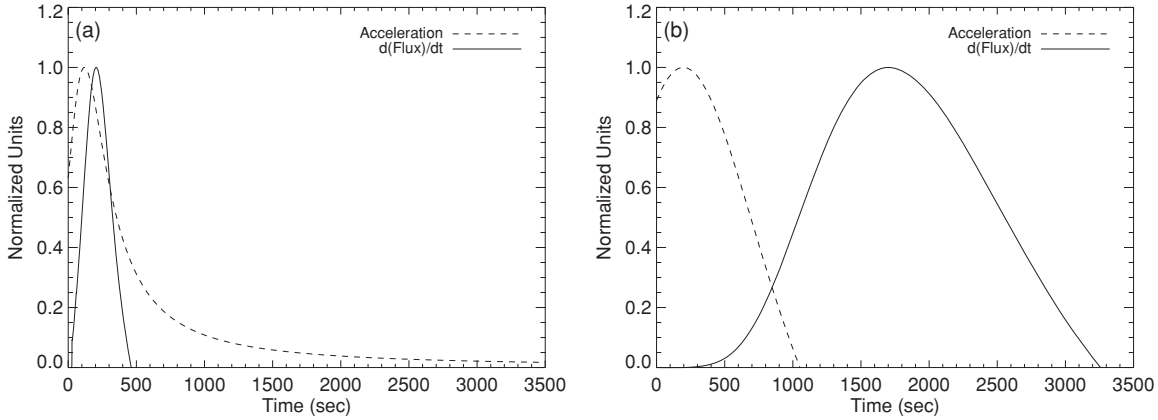

Figure 4. Acceleration of the flux rope (dotted lines) and flare light curve derivative (solid lines) for (a) $M_A = 1$, $B = 50$ G and (b) $M_A = 0.001$, $B = 10$ G.

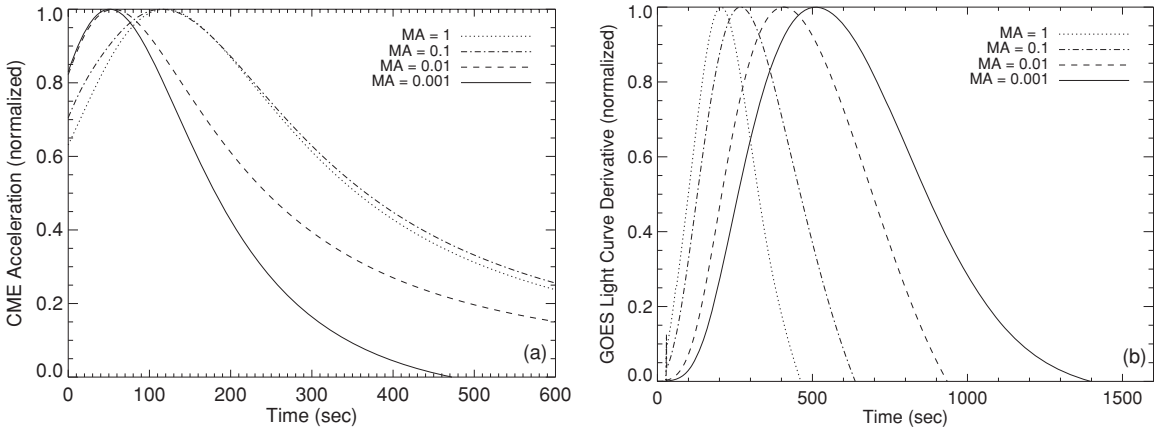

Figure 5. (a) Flux rope acceleration profiles and (b) derivatives of simulated light curves for a 50 G background field and varying values of M_A. Line styles indicate the different Mach numbers, as in Figure 2.

light curve derivative is consistent with observations for weak events.

In Figure 5, we show the acceleration profiles of the flux rope and the derivative of the *GOES* light curves for a constant background magnetic field (50 G) and varying values of M_A. Figure 5(a) shows that as the reconnection rate is increased, the acceleration peaks later in time. The CME acceleration is affected by the current sheet, which exerts a downward force on the flux rope. The slower the reconnection rate, the longer the current sheet, and the stronger this downward force will be, causing a deceleration that shifts the CME acceleration peak earlier. Fast reconnection rates lead to short current sheets and less deceleration, so the CME acceleration peaks later (Reeves 2006).

Figure 5(b) shows that increasing the reconnection rate has the opposite effect on the light curve derivative, causing it to peak earlier. This effect happens because the energy release is more sustained for cases with a slower reconnection rates, causing hot, dense loops that contribute significantly to the soft X-ray emission to be created well after the initiation of the flare. For cases with a fast reconnection rate, on the other hand, the energy release is more impulsive, leading to hot dense loops initially, but cooler and less dense loops as the flare evolves. Most of the contribution to the soft X-ray emission is from these initial hot, dense loops, and the light curve derivative peaks earlier.

The reconnection rate thus affects the timing of the peaks in the acceleration and the light curve derivative in opposite ways. A fast reconnection rate leads a smaller downward force on the CME due to the current sheet, allowing the CME acceleration to peak later, but it also causes a more impulsive energy release, which leads to an earlier peak in the soft X-ray derivative curve. Since the CME acceleration tends to peak before the light curve derivative, this effect leads to better correlation between the timing of the peaks for faster reconnection rates.

3.2. Relationship Between Flare Thermal Energy and Soft X-ray Emissions

In order to further understand the behavior of the soft X-ray light curves shown in Figure 5(b), we examine the thermal energy release rate, which also peaks at earlier times when M_A is increased. The thermal energy release rate is proportional to the Poynting flux carried into the current sheet in this model, and thus depends on the behavior of both the electric and magnetic fields in the current sheet. The net effect is that faster reconnection leads to short, high current sheets that contain lower field strengths, causing the thermal energy to peak earlier with increasing M_A (as detailed in Reeves 2006).

Even though an increase in the reconnection rate causes both the light curve derivative and the thermal energy release rate to peak at earlier times, we find that for the majority of the modeled cases, these two quantities are not well correlated with each other. Figure 6 shows a plot of the time difference between the peak in the thermal energy release rate and the peak of the light curve derivative for all of the cases studied. In particular, we find that in cases where the reconnection rate is slow and the

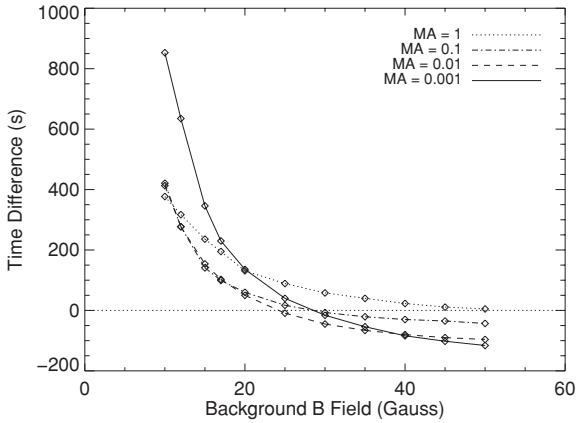

Figure 6. Delta time between the peaks of the thermal energy release rate and the *GOES* soft X-ray light curve derivative for all the cases studied. Line styles are the same as in Figure 2. Negative values indicate that the thermal energy release peaks before the light curve derivative.

background magnetic field is weak, there is a significant time difference between the peaks in these two quantities. Thus, the derivative of the soft X-ray light curve is not necessarily a good proxy for the energy release rate, especially in weak events.

We next examine the relationship between the total thermal energy input into each simulated flare and the resulting peak *GOES* 1–8 Å flux. This relationship is a key component of the theoretical explanation of the Neupert effect, where it is often assumed that peak soft X-ray flux, F, is proportional to the total thermal energy input, E, into the flare (e.g., Lee et al. 1995). Figure 7 shows plots of the peak *GOES* flux as a function of total thermal energy input, grouped together by reconnection rate. We find that in the modeled cases, F is not directly proportional to E, but rather there is a very good power-law relationship such that $F \sim E^{\alpha}$, with α in the range ~1.5–2.5, depending on the reconnection rate. Note that some of the flares modeled in Figure 7 are too small to be seen with the current *GOES* instrumentation, but they could be seen by a more sensitive instrument, such as the Solar Photometer in X-rays (SphinX) spectrometer (Sylwester et al. 2008) on the *CORONAS-Photon* mission.

Warren & Antiochos (2004) found that for a single loop modeled with a 1D hydrodynamic code,

$$F \sim \frac{E^{1.75}}{V^{0.75} L^{0.25}}, \tag{6}$$

where E is the total energy in the loop, V is the volume of the loop, and L is the loop length. We find that the individual loops in our simulations adhere very well to this relationship. The flares we model consist of about 500 loops with different lengths and volumes, so it is not surprising that the total thermal energy in the flare has a slightly different relationship to the peak soft X-ray flux than that predicted by Warren & Antiochos (2004).

The spectral index α is plotted as a function of reconnection rate in Figure 8. As the reconnection rate decreases, α becomes closer to 1. The spectral index is very close to linearly related to the log of the reconnection rate, though there is an indication that the line is flattening out at very slow reconnection rates.

4. DISCUSSION AND CONCLUSIONS

We have modeled 44 different flares with a wide range of background magnetic fields and reconnection rates. We find that, for a particular reconnection rate, the peak acceleration and the peak *GOES* flux are well correlated by a power-law relationship. This result is consistent with the observations (Maričić et al. 2007) and points to differing reconnection rates as a possible contribution to the scatter in the observed data.

We examine the timing between the peak of the acceleration and the peak of the derivative of the soft X-ray light curve, since many authors have found that the time profiles of these two quantities are similar. We find that the peaks in these curves are closest together when the background magnetic field strength is high and the reconnection rate is fast. These results are at

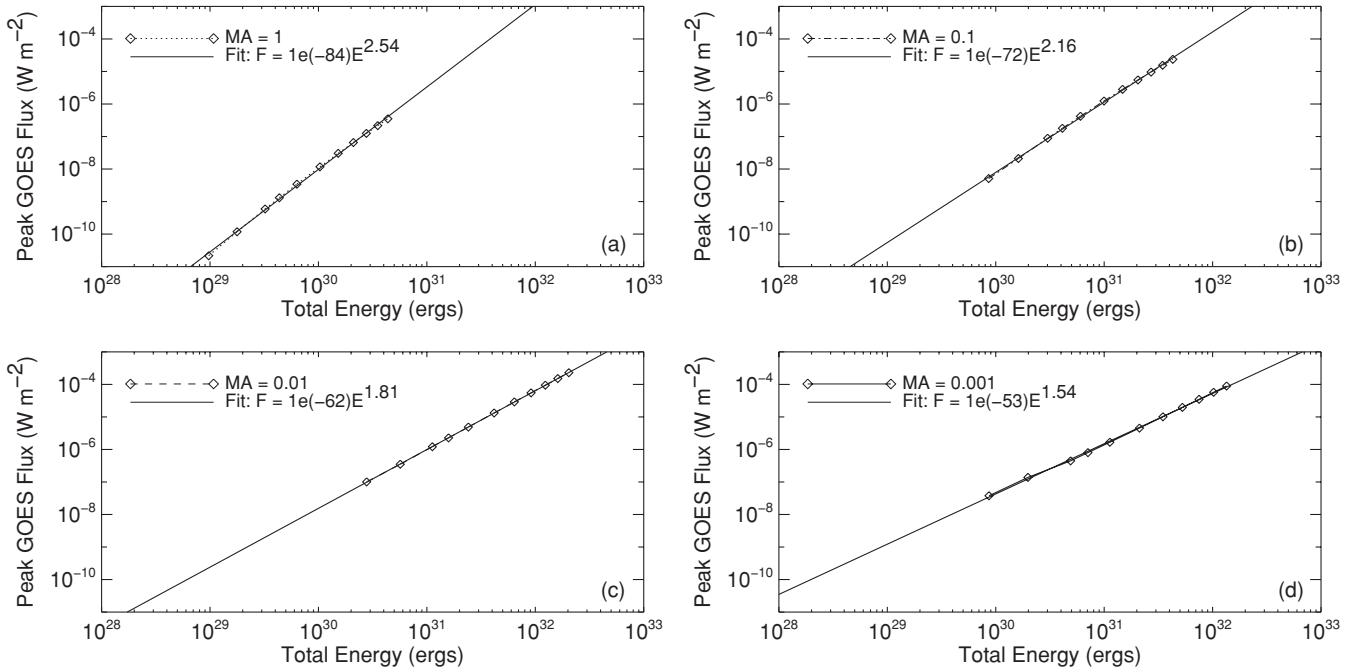

Figure 7. Peak *GOES* flux as a function of total thermal energy for (a) $M_A = 1$, (b) $M_A = 0.1$, (c) $M_A = 0.01$, and (d) $M_A = 0.001$. Also plotted is a power-law fit for each value of M_A.

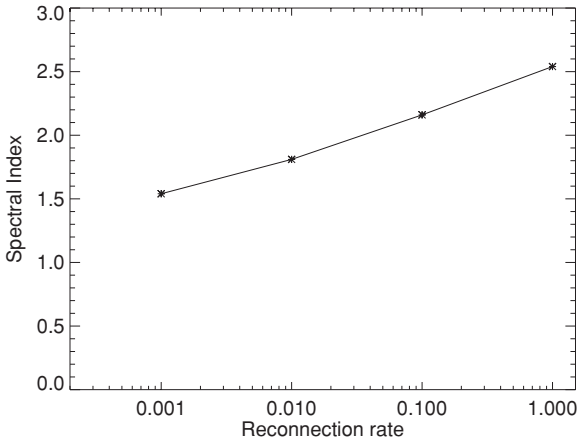

Figure 8. Spectral index from the fits in Figure 7 as a function of reconnection rate.

least somewhat consistent with observations. For example, the two events observed by Qiu et al. (2004) that have correlated acceleration profiles and light curve derivatives are large flares (*M* and *X* class), and thus have large background magnetic field strengths. Cases where the acceleration and the light curve derivative are not correlated are often due to eruptions that occur in weak field regions (e.g., Zhang et al. 2001; Maričić et al. 2007).

Reconnection rates, however, are more difficult to ascertain observationally. Several authors have found correlations between the reconnection electric field, E_z, and the light curve derivative (Qiu et al. 2004; Jing et al. 2005), but in order to relate this quantity to M_A, the Alfvén speed and the coronal magnetic field (or, alternatively, the thermal energy release rate, see Isobe et al. 2005) must be known. These quantities are difficult to observe, and there are only a few cases of direct observations of the reconnection inflow (Yokoyama et al. 2001; Lin et al. 2005; Narukage & Shibata 2006).

Using our modeled flares, we establish the relationship between the total thermal energy input into the flare (E) and the resulting peak *GOES* flux (F) to determine if our modeled flares follow the $F \propto E$ relationship expected in flares that exhibit the Neupert effect. We find that for our set of multi-stranded flares, F is not proportional to E, but rather these two quantities are very well represented by a power law of the form $F = E^{\alpha}$, where α decreases toward one with decreasing reconnection rate. This relationship is very similar to that found by Warren & Antiochos (2004) for a single loop model, and thus our results counter their speculation that the multi-stranded nature of flares could restore the $F \propto E$ behavior even though individual strands do not adhere to this relationship.

Typically, larger flares, such as *M* and *X* class flares, are more likely to emit X-rays in a manner consistent with the Neupert effect (Dennis & Zarro 1993; McTiernan et al. 1999; Veronig et al. 2002). In the model we employ, slower reconnection rates generally produce larger flares (given the same background magnetic field) because a high proportion of the released magnetic energy goes into thermal energy (Reeves & Forbes 2005) when the reconnection rate is slow. It is possible that eruptions with fast reconnection rates do not produce large flares very often since much of the released energy is used to drive the mass in the erupting CME. This circumstance would lead to a statistical population of large flares with low values of α so that they have a peak flux to energy relationship closer to that expected in the Neupert effect.

This model does not include the effects of hard X-ray producing particle acceleration, so we currently cannot make any predictions about the effect of the reconnection rate on the hard X-ray light curve, but correlations have recently been found between the CME acceleration and the hard X-rays emitted in associated flares (Temmer et al. 2008). It may be that the hard X-ray light curve is a better proxy for the energy release profile than the soft X-ray derivative. We plan to investigate this connection further by coupling the loss-of-equilibrium model with the flare loop model of Winter (2009), which incorporates the effects of non-thermal particles.

The authors thank the anonymous referee for helpful comments on the manuscript. K.K.R. is supported under the NSF-SHINE program, grant number ATM-0752257. S.J.M. is supported under the NSF-REU solar physics program at CfA, grant number ATM-0851866.

REFERENCES

Aschwanden, M. J., & Alexander, D. 2001, Sol. Phys., 204, 91
Burkepile, J. T., Hundhausen, A. J., Stanger, A. L., St. Cyr, O. C., & Seiden, J. A. 2004, J. Geophys. Res. (Space Phys.), 109, 3103
Cargill, P. J., Mariska, J. T., & Antiochos, S. K. 1995, ApJ, 439, 1034
Dennis, B. R., & Zarro, D. M. 1993, Sol. Phys., 146, 177
Dere, K. P. 1996, ApJ, 472, 864
Gallagher, P. T., Lawrence, G. R., & Dennis, B. R. 2003, ApJ, 588, L53
Harrison, R. A. 2003, Adv. Space Res., 32, 2425
Hori, K., Yokoyama, T., Kosugi, T., & Shibata, K. 1997, ApJ, 489, 426
Hori, K., Yokoyama, T., Kosugi, T., & Shibata, K. 1998, ApJ, 500, 492
Isobe, H., Takasaki, H., & Shibata, K. 2005, ApJ, 632, 1184
Jing, J., Qiu, J., Lin, J., Qu, M., Xu, Y., & Wang, H. 2005, ApJ, 620, 1085
Klimchuk, J. A., Patsourakos, S., & Cargill, P. J. 2008, ApJ, 682, 1351
Lee, T. T., Petrosian, V., & McTiernan, J. M. 1995, ApJ, 448, 915
Lin, J., & Forbes, T. G. 2000, J. Geophys. Res., 105, 2375
Lin, J., Ko, Y.-K., Sui, L., Raymond, J. C., Stenborg, G. A., Jiang, Y., Zhao, S., & Mancuso, S. 2005, ApJ, 622, 1251
Maričić, D., Vršnak, B., Stanger, A. L., Veronig, A. M., Temmer, M., & Roša, D. 2007, Sol. Phys., 241, 99
McTiernan, J. M., Fisher, G. H., & Li, P. 1999, ApJ, 514, 472
Moon, Y.-J., Choe, G. S., Wang, H., Park, Y. D., Gopalswamy, N., Yang, G., & Yashiro, S. 2002, ApJ, 581, 694
Narukage, N., & Shibata, K. 2006, ApJ, 637, 1122
Neupert, W. M. 1968, ApJ, 153, L59
Qiu, J., Wang, H., Cheng, C. Z., & Gary, D. E. 2004, ApJ, 604, 900
Reeves, K. K. 2006, ApJ, 644, 592
Reeves, K. K., & Forbes, T. G. 2005, ApJ, 630, 1133
Reeves, K. K., & Warren, H. P. 2002, ApJ, 578, 590
Reeves, K. K., Warren, H. P., & Forbes, T. G. 2007, ApJ, 668, 1210
Serio, S., Reale, F., Jakimiec, J., Sylwester, B., & Sylwester, J. 1991, A&A, 241, 197
Sterling, A. C., & Moore, R. L. 2005, ApJ, 630, 1148
Sylwester, J., Kuzin, S., Kotov, Y. D., Farnik, F., & Reale, F. 2008, JA&A, 29, 339
Temmer, M., Veronig, A. M., Vršnak, B., Rybák, J., Gömöry, P., Stoiser, S., & Maričić, D. 2008, ApJ, 673, L95
Veronig, A., Vršnak, B., Dennis, B. R., Temmer, M., Hanslmeier, A., & Magdalenić, J. 2002, A&A, 392, 699
Vršnak, B., Maričić, D., Stanger, A. L., & Veronig, A. 2004, Sol. Phys., 225, 355
Vršnak, B., Sudar, D., & Ruždjak, D. 2005, A&A, 435, 1149
Warren, H. P. 2006, ApJ, 637, 522
Warren, H. P., & Antiochos, S. K. 2004, ApJ, 611, L49
Warren, H. P., & Doschek, G. A. 2005, ApJ, 618, L157
Winter, H. D. I. 2009, PhD thesis, Montana State Univ.
Yokoyama, T., Akita, K., Morimoto, T., Inoue, K., & Newmark, J. 2001, ApJ, 546, L69
Zhang, J., Dere, K. P., Howard, R. A., Kundu, M. R., & White, S. M. 2001, ApJ, 559, 452
Zhang, J., Dere, K. P., Howard, R. A., & Vourlidas, A. 2004, ApJ, 604, 420